GEOLOGY OF THE NORTHEASTERN FLANK OF APOLLINARIS MONS, MARS: CONSTRAINTS ON THE EROSIONAL HISTORY FROM MORPHOLOGY, TOPOGRAPHY AND CRATER POPULATIONS.

Frank C. Chuang, David A. Crown, and Daniel C. Berman, Planetary Science Institute, 1700 E. Ft. Lowell Road, Suite 106, Tucson, AZ 85719 USA (chuang@psi.edu).

Introduction: Volcanic landforms on Mars have been noted since the earliest days of Martian exploration with ~60% of the surface covered by volcanic materials [1-7]. The lower surface gravity and atmospheric pressure of Mars compared to Earth are thought to favor explosive eruptive styles [8]. Studies of the morphometric properties of Martian volcanoes, such as the larger shields, tholi and paterae, have provided constraints on eruption styles and magnitudes through comparisons to terrestrial and other planetary volcanic landforms [9-13].

As higher-resolution data have been acquired over the past two decades, a more detailed understanding of the formation and degradation of Martian volcanoes is emerging [14-17]. In this study, we focus on the geologic history of the northeastern flanks of Apollinaris Mons (formerly Apollinaris Patera; center: ~9.2°S, 174.8°E). Using high-resolution datasets, we investigate the morphologic and topographic characteristics of the surface to produce a geologic map, as well as derive age constraints for geologic units from crater populations.

Background: Apollinaris Mons is a ~5.4 km high, ~190 km wide volcano with a 73 x 85 km summit caldera complex [11]. It is bordered to the north by the Medusae Fossae Formation and has been investigated as a source for fine-grained friable deposits in nearby equatorial regions of Mars [18]. Apollinaris Mons is also a potential source for lava flows that traveled southeast into Gusev Crater [19-21]. Spectral data covering the floor of Gusev indicates that outcrops and surficial materials are consistent with basalt [20] and that they are olivine-rich [22].

Past studies of Apollinaris Mons indicate a complex history of volcanism and hydro-volcanic activity. Detailed mapping suggested that ancient, large-scale explosive volcanic activity formed the main edifice and that the large, gently-sloping apron extending 140 km southeast beyond the caldera was formed by later, low eruptive rate lavas [23-24]. A more recent study interpreted the apron as emplaced lahars due to drainage of a caldera lake [25]. Other features of interest include incised valleys on the western flank and fluidized crater ejecta on flank surfaces. Significant questions remain as to the volcanic chronology and relative amounts of effusive and explosive materials, as well as the degree and styles of flank degradation.

Data and Methods: Thermal Emission Imaging System (THEMIS) day-time infrared data (dTIR; 100m/pixel) served as the regional basemap and night-time infrared data (nTIR; 100 m/pixel) provided a first-order proxy of thermal inertia for surface materials [26]. Gridded Mars Orbiter Laser Altimeter (MOLA; ~463 m/pixel) data served as the regional topographic basemap and individual Precision Experiment Data Record (PEDR) altimetry tracks provided profile-ready data. Geologic mapping utilized multiple grayscale Context Camera (CTX; ~5-6 m/pixel) images with individual HiRISE images (~0.25 m/pixel) providing high-resolution views of select areas and stereo-derived DTM data. All datasets were imported into ArcGIS Desktop 10.4 (ArcGIS) software for digital mapping, topographic analysis, and crater counting. Compilation of crater size-frequency distributions (CSFD) for geologic units was done using CraterTools 2.1 for ArcGIS [27].

Geologic Units and Features: We have identified and described eight geologic units in the NE Apollinaris Mons study region (Figure 1). Units are characterized by their morphology, texture, thermophysical signatures (nTIR and dTIR), and their contact relationship(s) with adjacent units. Three units form a sequence that collectively represent Apollinaris Mons flank deposits: Apollinaris Mons upper flank (*Amfu*), Apollinaris Mons mid-flank (*Amfm*), and Apollinaris Mons lower flank (*Amfl*) materials. Other units include mantling material (*m*), Medusae Fossae Formation - lower member (*Mfl*) [28], knob (*k*), plains material (*p*), and crater material (*c*).

Amfu material appears massive and generally occurs in the form of plateaus, ridges, and knobs that represent well-preserved sections of volcanic flank deposits, potentially representing the early formation of Apollinaris Mons. *Amfm* and *Amfl*, both positioned below *Amfu*, are portions of flank deposits that have been modified by erosional processes. *Amfm* appears rough-textured with local channel-like incisions, whereas *Amfl* is smooth and extends to the base of the volcano. Numerous large troughs present within *Amfl* may be possible pathways for downslope sediment transport. *Amfm* and *Amfl* surfaces exhibit similar brightness in nTIR data and they both likely experienced similar erosional processes. Areas below Apollinaris flank units and beyond are covered mainly by *p*, *m* and *Mfl* materials. Both *m* and *Mfl* are rough-textured and appear heavily eroded by eolian activity

with numerous small knobs or yardangs aligned with the NE-SW wind direction. Plains materials are relatively flat beyond the volcano base and contain small areas of clustered knobs, *k*. Impact craters and their lobate ejecta deposits, *c*, form the highest stratigraphic unit covering the eastern third of the study region and other localized areas.

HiRISE stereo pair PSP_001645_1725 and PSP_002634_1725 cover a spur-like ridge extending downslope from an *Amfu* plateau and adjacent *Amfl* materials. *Amfu* appears rough and craggy with interspersed smooth, low-lying areas, some with dune fields. Abundant small impact craters, including clusters of background secondaries, indicate long-term exposure of this unit at the surface. In some locales along *Amfu* scarps, linear features with shadowed slopes reaching several tens of meters to ~330 m in length are aligned parallel to the downslope direction; possible joints within *Amfu* flank deposits.

In CTX images, small impact craters ~15 m to ~120 m (geom. mean ~33 m) in diameter with ejecta deposits raised above the surrounding terrain are observed in each geologic unit in the study region. These small rampart craters indicate the presence of volatiles either within the shallow subsurface or in the atmosphere at the time of impact [29-30]. Unit *Amfu* has the highest density (craters/km^2) followed by units *c*, *Amfl*, *p*, *Amfm*, *m*, *k*, and *Mfl*.

Erosion of Flank Materials: The position of *Amfu* plateaus above *Amfm* and *Amfl* surfaces, and the high relief along *Amfu* plateau margins, indicates past erosion and removal of volcanic flank materials. From multiple PEDR tracks, the overall volcano slope is ~3°-3.5° with a minimum of ~100 m relief along downslope-facing *Amfu* plateau scarps. To estimate the area and potential volume of material that previously surrounded *Amfu* plateaus, ridges, and knobs, we subtracted the flank slope from MOLA data using a second-order polynomial interpolated surface. We also excluded high residuals areas, selected high and low bounds, and masked out small outlying knobs and the interior of a 6 km diameter crater within the synthetic surface. From the ~1,625 km^2 slope-corrected surface, we selected an appropriate "fill" level that accounts for all areas likely to be occupied by former flank material. For the study region, we estimate that ~8,632 km^3 of pre-eroded flank material has been removed, well below one percent of the total volume of Apollinaris Mons [11].

Future Work: Results from our geologic mapping and related studies, combined with modeled ages for each geologic unit, will be used to further assess the geologic history of the study region. We will also complete ongoing analyses using CTX and HiRISE images to further investigate the distribution of rampart craters and volcanic joints across Apollinaris Mons.

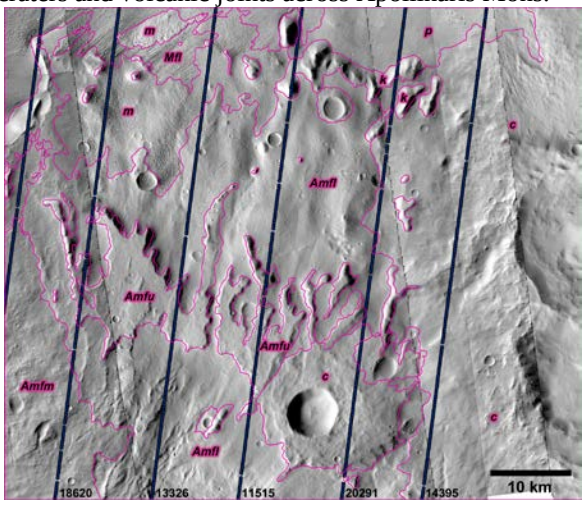

Figure 1. CTX images covering the NE Apollinaris Mons study region with mapped geologic units (outlined in magenta) and PEDR profiles (blue dots).

References: [1] McCauley, J.F. et al. (1972) *Icarus, 17*, 289-327. [2] Carr, M.H. (1973) *JGR, 78*, 4049-4062. [3] Plescia, J.B. and Saunders, R.S. (1979) *Proc. LPSC 10*, 2841-2859. [4] Greeley, R. and Spudis, P.D. (1981) *Rev. Geophys., 19*, 13-41. [5] Mouginis-Mark, P.J. et al. (1992) *Mars, UA Press*, 424-452. [6] Scott, D.H. and Carr, M.H. (1978) *USGS Map I-1083*. [7] Tanaka, K. et al. (2013) *USGS Sci. Invest. Map 3292*, [8] Carr, M.H. (2006) *Cambridge Univ. Press*, 307 p. [9] Pike, R.J. (1978) *Proc. LPSC 9*, 3239-3273. [10] Hodges, C.A. and Moore, H.J. (1992) *USGS Prof. Paper 1534*, 194 pp. [11] Plescia, J.B. (2004) *JGR*, 109, doi:10.1029/2002JE002031. [12] Crown, D.A. et al. (2010) *LPSC 41*, Abstract #2225. [13] Crown, D.A. et al. (2011) *LPSC 42*, Abstract #2352. [14] Bleacher, J.E. et al. (2007) *JGR, 112*, doi:10.1029/2006JE002873. [15] Williams, D.A. et al., (2009) *PSS, 57*, 895-916. [16] Hauber, E. et al. (2011) *GRL, 38*, doi:10.1029/2011GL047310. [17] Platz, T. et al. (2011) *EPSL, 312*, 140-151. [18] Kerber, L. et al. (2012) *Icarus, 219*, 358-381. [19] Greeley, R. et al. (2005) *JGR, 110*, doi:10.1029/2005JE002401. [20] Martinez-Alonso, S. et al. (2005) *JGR, 110*, doi:10.1029/2004JE003041. [21] Lang, N.P. et al. (2010) *JGR, 115*, doi:10.1029/2009JE003397. [22] McSween, H.P. et al. (2006). [23] Robinson, M.S. et al. (1993) *Icarus, 104*, 301-323. [24] van Kan Parker, M. et al. (2010) *EPSL, 294*, 411-423. [25] El Maarry, M.R. et al. (2012) *Icarus, 217*, 297-314. [26] Fergason, R. et al. (2006) *JGR, 111*, doi:10.1029/2006JE002735. [27] Kneissl, T. et al. (2010) *LPSC 41*, Abstract #1638. [28] Greeley, R. and Guest, J.E. (1987) *USGS Map I-1802B*. [29] Barlow, N.G. (1994), *JGR, 99*, 10,927-10,935. [30] Boyce, J.M. et al. (2000) *LPSC 31*, Abstract #116.